Epitaxy and domain growth of Pb on Ni(001)

Teddy Tse, Peter W Stephens and Peter J Eng†

Department of Physics, State University of New York, Stony Brook, NY 11794, USA

Abstract. We study the growth of the $c(2\times2)$ structure of Pb on Ni(001) with high-resolution x-ray diffraction. By monitoring the adsorbate–substrate and the adsorbate–adsorbate interference diffraction peaks, we are able to determine the registry and growth process of the first overlayer. Pb atoms change from hollow site to non-hollow site growth as coverage increases. Results at higher substrate temperatures indicate a different growth process at low coverage. We propose a model of adsorbate aggregation at sites in line with Ni atoms around pinning centres to account for the observed results.

1. Introduction

An understanding of thin-film growth under various conditions is of interest to technology and basic sciences. In this regard, it is important to know the atomic structure of epitaxial layers. Recently, x-ray diffraction has been growing in importance for such experiments [1]. In this paper, we report experiments that employ high-resolution x-ray diffraction as a technique to probe the structure of an epitaxially grown monolayer during its process of deposition. A novel feature of the present work is the application of diffraction techniques to the determination of the structure of an adsorbed phase at sufficiently small domain size that it can only be observed via its interference with the substrate.

The evolution of domains on surfaces depends upon adsorbate coverage, time, temperature, and impurity content. One expects that the adsorption site degeneracy would have a significant influence on domain growth processes. Yet, there has been relatively little attention placed on such issues [2, 3]. In the present experiments on a twofold-degenerate domain structure, we study how the growth of surface coherence is limited by antiphase domain boundaries as the coverage approaches that of an ideal monolayer.

2. Experimental details

The experiments were performed at the State University of New York X3B2 bending magnet beamline at the National Synchrotron Light Source. A 6 mrad fan of 11 keV x-rays was sagitally focused by two Si(111) crystals at the sample [4] in grazing incidence geometry. A Ge(111) crystal was used to analyse the vertically scattered beam giving a longitudinal instrumental resolution of $0.000\,82$ Å^{-1} full width at half maximum (FWHM) as determined from a well annealed $c(2\times2)$ structure of Pb on the current Ni sample at 450 °C. The sample was held in an ultrahigh-vacuum (UHV) system with a base pressure of 6×10^{-11} Torr. The UHV chamber was equipped with a double-pass cylindrical mirror analyser for Auger electron

† Current address: Department of Physics, University of Illinois, Urbana, IL 61801, USA

spectroscopy (AES), a quadrupole residual gas analyser, reverse reading low-energy electron diffraction (LEED), a sputter gun, and an oven for Pb deposition.

The Ni sample used had a mosaic of 0.15° FWHM and a surface miscut of 0.025°C [5]. The sample cleaning process started with Ar ion bombardment below 100 °C to remove all surface impurities on the surface, particularly C, which segregates on the surface at lower temperatures [6]. Then the sample was annealed at 680 °C for 10 min.

As the sample was cooling, C started to appear once the temperature dropped below 600 °C. At about 420 °C, 1–2% C had segregated onto the surface. Further cooling to the substrate deposition temperature did not show any increase in contamination. It is known that by exposing a surface to O, one can reduce the extent of C contamination. Hence we tried an alternative cleaning process by starting with Ar ion sputtering, following by flashing the sample to 680 °C. At 550° we removed C by exposing the sample to O for 1 min, then annealed the sample at 680 °C to remove the adsorbed O. Repeated cycles of O exposure and annealing depleted the C diffused from the bulk, but led to the grown of S on the surface. Therefore, we limited ourselves to only one or two O cycles in the cleaning process. Compared to the previous cleaning cycle, C segregated more slowly during the cooling process, yet the final level of C contamination remained the same below 200 °C.

Pb was deposited by evaporation from a quartz crucible, resistively heated to 620°. A shutter controlled the amount evaporated onto the sample that was held at a fixed temperature. Chamber base pressure during Pb deposition was below 1×10^{-9} Torr. We used AES to determine the coverage and performed x-ray scans in between doses of about 0.1 half monolayer. Typically it took about 1.5 h to complete a run.

3. The Pb/Ni (001) system

The Pb c(2 × 2) structure on an Ni(001) substrate system under study has two possible sublattices that are thermodynamically equivalent as shown in figure 1. (Specific evidence for this fourfold adsorption site is given below.) An in plane diffraction peak $(hk0)$ is an allowed Ni bulk reflection if h and k are both even. Due to the truncation of a three-dimensional crystal, rods of scattering intensity occur perpendicular to the surface, passing through allowed bulk Bragg peaks. These crystal truncation rods produce measurable intensity at bulk forbidden positions [7, 8]. The x-ray intensity is sensitive only to the sample surface if both h and k are odd. In addition, the scattering amplitudes from Pb atoms in the two sublattices are in phase for $h + k$ even, and out of phase for $h + k$ odd. In the present work, we look at the (100) and (110) peak positions. Because of the out of plane focusing and broad detector, we have very low resolution in the (00ζ) direction, integrating approximately over the range $0 < \zeta < 0.05$ reciprocal lattice units. This resolution function gives an appropriate set-up for the present two-dimensional scattering. For simplicity, we will designate all surface $(hk\zeta)$ triplets in this paper as $(hk0)$ though ζ is in fact a small positive number.

The Pb c(2 × 2) phase diffracts at the Ni(100) position. Since there is no Ni crystal truncation rod intersecting at the (100) position, the diffraction peak measures the coherence, or the average domain size of the c(2 × 2) domains. The (100) diffraction is therefore sensitive only to adsorbate–adsorbate correlations.

Ni(110) is a bulk forbidden peak on the (001) surface that measures the coherence of the FCC surface structure. Pb atoms deposited on the surface will produce an interference with this substrate truncation rod. It is important to note that the interpretation of this interference between substrate and adsorbate is particularly simple for the case of x-ray
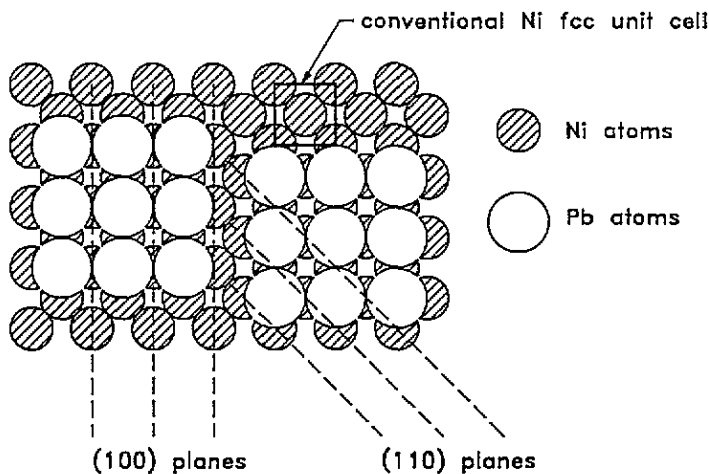
Figure 1. The structure of Pb c(2 × 2) phase on Ni(001) and the directions of (100) ordering peak and (110) non-ordering peaks. Two equivalent sublattices of Pb are shown.

diffraction, inasmuch as kinematic diffraction theory holds for the weak scattering process. This also gives sensitivity to Pb atoms for coverage that is too low to be observed by either electron or x-ray diffraction at adsorbate peaks. Since Pb atoms in either sublattice scatter with the same phase, the diffraction peak does not distinguish between Pb atoms in domains of different sublattices. Thus the (110) peak gives no direct information on the domain ordering, but it is sensitive to the total amount of Pb atoms that scatter coherently with the substrate.

The above peaks can be considered as complementary in examining the surface structure in the sense that one registers the locations of adsorbates with respect to the substrate while the other registers the locations of adsorbates with respect to one another. Hence we are able to obtain a detailed understanding by following both the (100) and (110) peaks during the deposition process.

We try various models to extract correlation lengths from lineshapes of diffraction peaks. The most successful is a Lorentzian to the $\frac{3}{2}$ power ($L^{3/2}$), which may be interpreted as an exponential decay of correlations in two dimensions,

$$\langle n(r)n(0)\rangle = \exp(-r/\xi) \tag{1}$$

where $n(r) = \pm 1$ and ξ is the correlation length. For the (100) peak, $n(r)$ depends on the sublattice of c(2 × 2) structure. For the (110) peak, $n(r)$ depends on the local height of the surface. In either case, a radial scan through the peak yields

$$I(q_\parallel) \propto (q_\parallel^2 + \xi^{-2})^{-3/2} \tag{2}$$

where $q_\parallel$ is the deviation from the in plane reciprocal lattice vector of the diffraction peak.

A fit to a Ni(100) scan from a clean starting substrate surface gives a correlation length of 920° Å. (Alternatively, one could describe the width as finite crystal size broadening and estimate a somewhat larger grain size of $2\pi/(0.00163 \text{ Å}^{-1}\text{FWHM}) = 3860$ Å.)

4. Experimental results

4.1. Room-temperature deposition

We first consider results for a monolayer of Pb at a substrate temperature of 32 °C. Figure 2 compares three surface signals as a function of Pb coverage: the (110) truncation rod intensity, the (100) diffraction peak width, and the 94 eV Pb AES signal. The data compiled in figure 2 were actually taken in two deposition cycles, with good agreement between each other. The x-ray intensities were stable for at least 25 min after each deposition, indicating that there was no annealing at this substrate temperature while data were being collected.
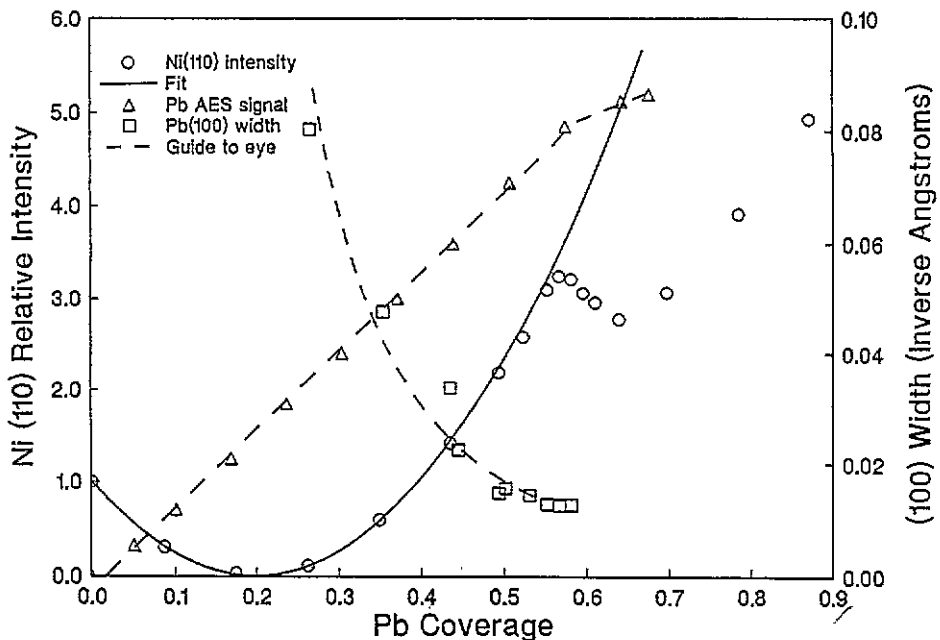

Figure 2. (110) relative intensity and (100) width as functions of Pb coverage. The solid line corresponds to fit from (2). The Pb AES signal is in arbitrary units. The broken lines are guides to the eye.

Calibration of Pb coverage was done by first depositing to different coverages, determined by AES, at room temperature and then heating up the system above 200 °C. The coverage at high temperature was observed to decrease asymptotically to a particular value. The same set-up was used for a related experiment that investigated the ordering kinetics of the same Pb/Ni(001) system with a non-conserved order parameter [9]. There we followed the growth of pure $c(2 \times 2)$ domains with the (100) diffraction peak after an upquench in temperature. The growth exhibited a scaling and power law behaviour with an exponent near 0.13. The same final coverage found in the ordering kinetics and the present desorption experiments gives confidence in our coverage calibration here. We defined this final coverage to be a half monolayer on the AES scale. This sets the horizontal scale in figure 2. In the following discussions, θ is the coverage of Pb atoms, defined to be unity if every adsorption site is occupied. The $c(2 \times 2)$ saturation coverage occurs at $\theta = 0.5$.

We study the ordering of the Pb monolayer with radial scans along (100) during the growth process. Representative data are shown in figure 3. The (100) ordering peak is first observable near a coverage of $\theta = 0.25$. The weak and broad (100) peak at low coverage implies that neighbouring adsorbed Pb atoms are poorly correlated into $c(2 \times 2)$ domains with $\xi \simeq 16$ Å. As the coverage is increased, the (100) peak width drops rapidly by a factor of 6.5 and saturates. A fit of $L^{3/2}$ convoluted with the resolution function gives the saturated coherence length of 80 Å. At the same time, the intensity at the peak increases by a factor of 70, indicating much more developed $c(2 \times 2)$ structures. The width of the peak is plotted against Pb coverage as squares in figure 2. Continuing to increase the Pb dose to $\theta = 0.64$, the (100) peak disintegrates and a new broad peak appears near $(1.13, 0, 0)$. As the deposition proceeds further, a weak and broad (100) peak reappears in coexistence with the one at $(1.13, 0, 0)$.
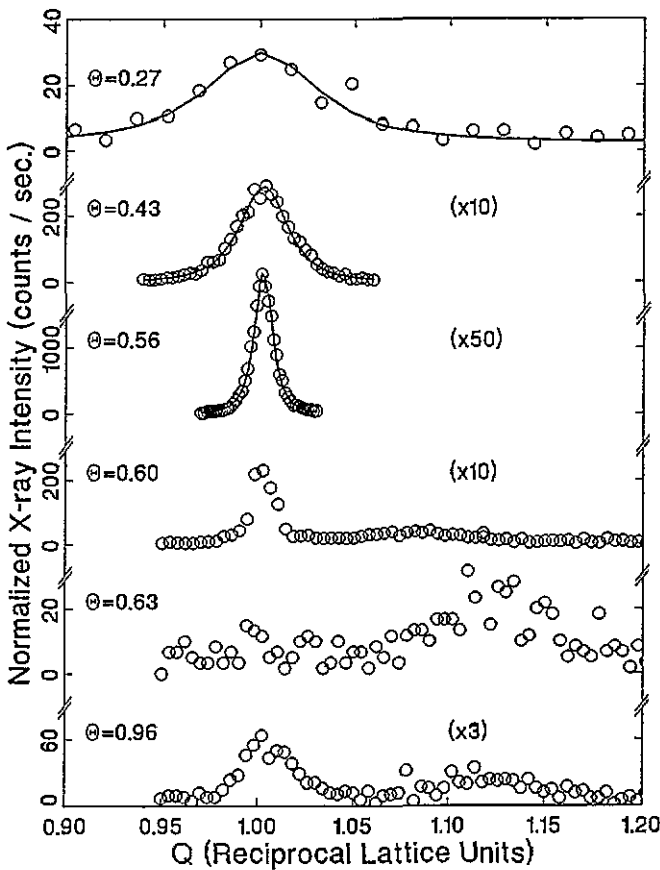

Figure 3. The evolution of the (100) peak with increasing Pb coverage from scans along the $(h00)$ direction. The lines are Lorentzian to $\frac{3}{2}$ fits.

In order to obtain additional information on the growth process, we study the (110) peak along with the (100) scans. $L^{3/2}$ convoluted with the resolution fits all (110) profiles well. Figure 4 shows scans with fits of a clean and a dosed surface. The width of the peak indicates a correlation length of 920 Å, the same as a clean Ni surface. Though the relative

intensities of the peaks throughout the Pb coverage range are different, they all exhibit the same lineshape and width.
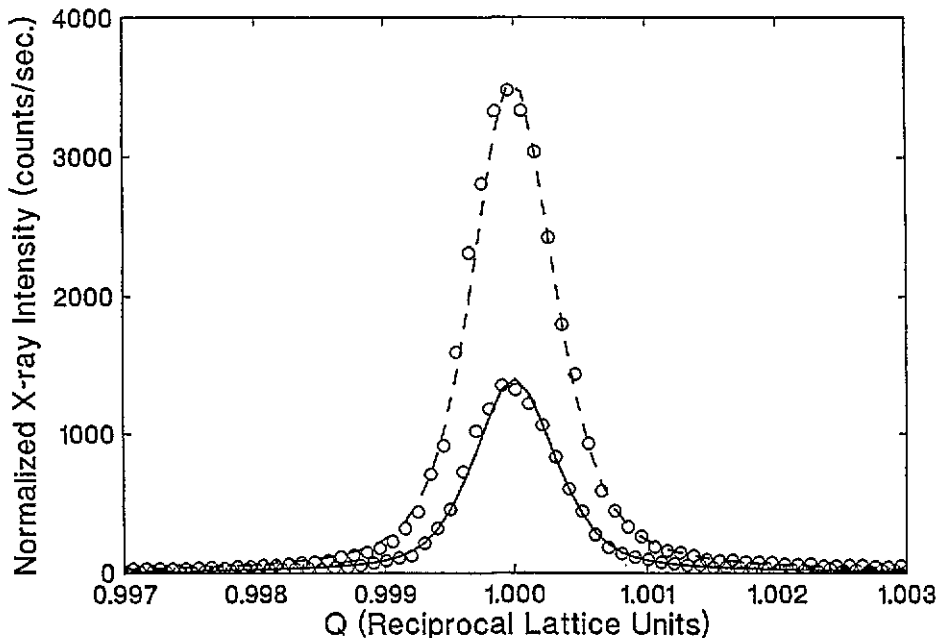

Figure 4. The (110) peak fitted with a Lorentzian to $\frac{3}{2}$ at 30 °C. The peak with a solid line is from a clean surface. The peak with a broken line is at $\theta = 0.49$.

The intensity of the (110) surface peak as a function of Pb coverage is plotted as circles in figure 2. We can understand the change of intensity with the following model. If Pb atoms adsorb in the fourfold-coordinated hollow sites, the scattering amplitude of the (110) peak is expected to be

$$A(\theta) \sim 2(\tfrac{1}{2})D_{Ni}f_{Ni} - 2\theta D_{Pb}f_{Pb} \tag{3}$$

where $f_{Ni} = 21.37$ and $f_{Pb} = 68.45$ are the atomic scattering factors of Ni and Pb respectively at $Q = 2.51\ \text{Å}^{-1}$. D_{Ni} and D_{Pb} are the Debye–Waller factors for bulk Ni and a Pb layer respectively. The first term accounts for the two Ni atoms in a two-dimensional Ni FCC unit cell with the surface truncation rod factor $\frac{1}{2}$ [8]. The second term accounts for the two Pb adsorption sites in the unit cell, which scatter out of phase with the Ni atoms. A factor of two takes into account that at a half monolayer there is one Pb atom per unit cell. Thus the relative intensity of a dosed surface to a clean surface at the (110) peak is

$$I(\theta)/I(0) = (1 - 2(D_{Pb}/D_{Ni})(f_{Pb}/f_{Ni})\theta)^2. \tag{4}$$

Further assuming a steady rate of deposition

$$\theta = rt \tag{5}$$

where r is the rate of deposition and t is the total time when the shutter of the Pb oven is open. We fit the data with $(D_{Pb}/D_{Ni})r$ as a single parameter as the solid line in figure 2.

The AES signal of Pb is plotted as triangles in arbitrary units. The linear increase justifies the assumption of constant deposition rate assumed in (5). A typical deposition rate is 0.1 half monolayer per minute. The good agreement at low coverage indicates that Pb atoms indeed adsorb in the hollow sites, scattering out of phase with the Ni atoms, thereby causing the initial drop in intensity. Other possible adsorption sites would lead to different behaviour of the data in figure 2. For example, if the Pb atoms adsorb atop Ni surface atoms, the relative (110) intensity would be

$$I(\theta)/I(0) = (1 + 2(D_{Pb}/D_{Ni})(f_{Pb}/f_{Ni})\theta)^2. \tag{6}$$

Pb atoms randomly distributed between the two bridge sites would make no changes to the clean Ni signal because the phases from two different sites cancel each other out. Pb atoms distributed equally into domains of only one particular bridge site would produce

$$I(\theta)/I(0) = 1 + ((D_{Pb}/D_{Ni})f_{Pb}/f_{Ni})^2(2\theta)^2. \tag{7}$$

All of these cases are clearly excluded by the data of figure 2.

With the calibration of coverage by AES, the data of figure 2 imply that the ratio D_{Pb}/D_{Ni} is significantly less than unity. If $D_{Pb}/D_{Ni} = 1$, the parabola should have a much stronger curvature than the solid line shown; we find D_{Pb}/D_{Ni} to be 0.78. This is a reasonable value because one would expect a weakly bound overlayer to have stronger thermal vibrations than a bulk surface due to less constraint from the third dimension. An alternative explanation is that the c(2 × 2) phase harbours a significant concentration of vacancies, so that the Pb amplitude is weaker than in (4).

As the coverage increases above $\theta = 0.5$, the intensity at the Ni(100) position starts to deviate from the model, indicating a change of growth mode. Evidently, beyond this point, some Pb atoms no longer adsorb in the hollow sites. We discuss these higher-coverage data below.

By tying the (100) and (110) results together, we are able to obtain a more complete picture of the growth process. At very low coverages the absence of (100) shows that no islands larger than a detectable limit of the order of 10 Å are formed, but the (110) peak shows that Pb atoms adsorb in the hollow sites. This can be interpreted as the Pb atoms, due to limited mobility, not being able to diffuse into islands. The structure is a quenched lattice gas. After reaching a coverage of $\theta = 0.25$, the probability of new Pb atoms landing sufficiently close to neighbouring sites increases. Pb atoms start to coalesce into islands until they come into contact with one another as shown by the drop and saturation in the (100) width. As the domains coalesce, the influence of the twofold-degenerated ordered state becomes relevant. If the colliding domains belong to the same sublattice, they merge into larger domains. If they belong to different sublattices, growth stops at the domain walls. Adding more Pb atoms induces strains in the structure and displaces some adsorbates into non-hollow sites, resulting in deviation of the (110) intensity from (4). When even more Pb atoms are added, they fill all the available hollow and non-hollow sites and the domains touch one another, terminating domain growth.

As the coverage is further increased, the c(2 × 2) structure is destroyed, though not completely. Apparently, new Pb atoms are attracted onto the surface sufficiently strongly that they themselves or the neighbouring atoms are forced out of the fourfold sites. A new structure is formed, showing up as a weak fractional-order diffraction peak at approximately $(1.13, 0, 0)$. The emergence of the new structure destroys the c(2 × 2) phase, resulting in the (110) intensity drop after reaching the cusp at $\theta = 0.57$. As coverage is further increased

beyond $\theta \geqslant 0.64$, the (110) intensity starts to grow again, and a weak, broad peak returns at the (100) position. The Ni(110) reflection corresponds to Pb(200) bulk reflection while the Ni(100) position corresponds to the Pb(100) truncation rod, suggesting multi-layer growth.

Similar fractional-order peaks were also observed in the ordering kinetics experiment mentioned above. Starting with a coverage above $\theta = 0.55$ at room temperature, x-ray scans along the (100) direction showed that above 200 °C, a peak at $(1.2, 0, 0)$ collapsed into a peak at $(1.14, 0, 0)$, which also collapsed eventually into a peak at $(1, 0, 0)$ as θ decreased toward 0.5. Other fractional peaks appeared at $(N/5, 0, 0)$ and $(N/7, 0, 0)$, where N is an even integer, along with $(1.14, 0, 0)$ and $(1.2, 0, 0)$ during the above evolution, suggesting that the phases were $c(5\sqrt{2} \times \sqrt{2})R45°$ and $c(7\sqrt{2} \times \sqrt{2})R45°$. Together with the AES measurements it seems clear that the saturated Pb layer starts with a $c(5\sqrt{2} \times \sqrt{2})R45°$ phase with the highest Pb density. Then it desorbs to the optimum coverage for a less dense $c(7\sqrt{2} \times \sqrt{2})R45°$ phase. Further desorption gives the ideal coverage, $\theta = 0.5$, of the $c(2 \times 2)$ phase. A roughly unchanged (110) peak before and after the unquench confirms that most Pb atoms are indeed in the fourfold hollow sites throughout the annealing process. The clear picture at high temperature implies that the fractional-order structure at room temperature is some mildly ordered $c(7\sqrt{2} \times \sqrt{2})R45°$ phase.

Summarizing the results for room-temperature deposition, we find that Pb atoms occupy the fourfold hollow sites with nearest-neighbour exclusion for $0 < \theta < 0.5$. The low end of this coverage range has a dilute structure, with no correlations beyond the excluded nearest neighbours. At higher coverages, a $c(2 \times 2)$ adsorbed phase is observed. The $c(2 \times 2)$ phase is destroyed for coverages above $\theta = 0.5$. These simple, plausible results give us confidence that the truncation rod inteference can be interpreted directly to determine adsorbate atomic structure.

4.2. High-temperature deposition

In comparison with the simple picture of Pb adsorption in fourfold-coordinated hollow sites at room temperature, we find more complicated behaviour in experiments in which Pb is dosed onto the Ni surface at elevated temperatures. Figure 5 shows the results of the normalized (110) intensity at various temperatures. At 70 °C the result is the same as that described above for 32 °C, but as the substrate temperature is raised above 75 °C, the (110) intensity does not follow the hollow site growth pattern when Pb atoms are first deposited on the substrate. At 100 °C, the intensity drops mildly at low coverages. As the coverage is increased, the intensity goes to zero at a coverage higher than that of 32 or 70 °C. At still higher temperatures, the intensity rises above that of a clean surface. As the Pb coverage is increased, the intensity decreases and follows a trend similar to that at room temperature, except that the intensity minimum is further displaced toward high coverages. AES spectra at different coverages throughout these dosing experiments show that the Pb signal increases and the Ni signal decreases in the same way as in the lower-temperature case. This shows that there is no desorption or bulk crystallite formation of Pb on the surface. Near $\theta = 0.58$ the Pb AES signal shows an abrupt decrease of slope while the (110) intensity increases montonically (not shown in figure 5), indicating multi-layer growth.

The increased (110) intensity at low coverages implies that the adsorbed Pb atoms are scattering (on average) in phase with the Ni surface atoms. At face value, this implies that the Pb atoms are not going into the same fourfold sites that were observed at lower dosing temperature. At the same time, we note that at each temperature there is a coverage at which the (110) intensity is zero, i.e., the adsorbed Pb atoms scatter x-rays destructively with the Ni substrate. This can only occur if the majority of the Pb atoms are located in
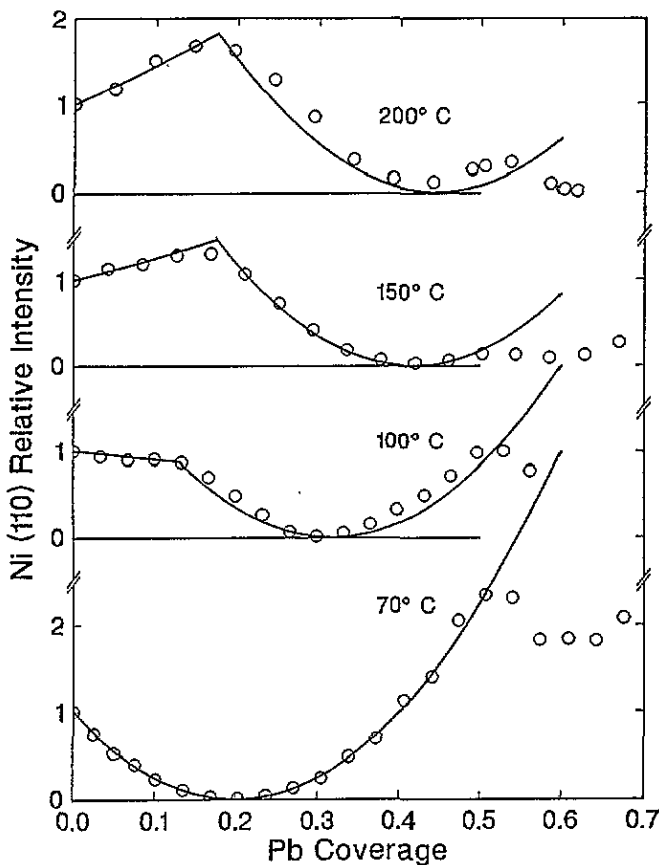
Figure 5. The (110) relative intensity as a function of Pb coverage at various temperatures.

the fourfold hollow sites. One simple resolution of this apparent contradiction is discussed below.

In order to investigate the difference between the initial growth modes above and below 75 °C, we varied the temperature at a coverage less than $\theta = 0.15$ after dosing. When a surface is dosed at 100 °C and then cooled below 70 °C, the (110) intensity remains fixed at the 100 °C levels shown in figure 5. However, when a surface initially dosed at 60 °C is raised to 100 °C, the (110) intensity increases to the high-temperature trace of figure 5. This irreversible behaviour of the (110) interference suggests that the difference between high- and low-temperature structures is a kinetic effect. At high temperature, the Pb atoms are able to diffuse some distance on the surface, to the most favourable adsorption sites, whereas below 75 °C, they travel a much shorter distance, only to the nearest island.

At a higher coverage, $\theta = 0.47$, an increase in temperature from 100 °C to 350 °C drives the (110) intensity to the level of the 70 °C data while AES shows that no Pb atoms desorb. This indicates that near the saturation coverage, the system relaxes to the same fourfold-coordinates c(2 × 2) sites that are populated when it is dosed at or below 70 °C.

The growth of the c(2 × 2) domains is similar to the lower-temperature ordering, but displaced to higher coverages. Indeed, the (100) peak starts to appear around the minimum of the (110) intensity curve. Then the (100) peak width reduces to no less than 75% of its

initial value before it disintegrates at $\theta = 0.5$. Afterwards a fractional-order peak develops at about $(1.16, 0, 0)$ through the destruction of the c(2 × 2) phase. It seems that there are two separate mechanisms operating during the higher-temperature growth. The first accounts for the low-coverage growth with an increase in the (110) intensity. The second mechanism, namely island growth, starts to dominate when the (110) intensity curve turns around towards its minimum. The c(2 × 2) domains grow until the completion of a half monolayer, oversaturate to a higher-density phase, and then follow multi-layer growth.

One possible mechanism that explains the initial increase of the (110) intensity is the aggregation of Pb atoms around pinning sites such as step edges or Ni surface vacancies. A similar experiment of Pb on a Cu(001) surface without C exhibiting the same high-temperature behaviour [10] indicates that the C impurities on the Ni substrate surface do not serve as pinning sites. Without a detailed microscopic picture, we may still hypothesize the presence of some pinning sites that favour Pb atoms adsorbing at sites in line with the surface Ni atoms such as Ni vacancies or atop sites (abbreviated as Ni sites below). When the substrate temperature is above a particular value, 75 °C from our results, we assume that the Pb atoms acquire sufficient thermal energy such that a fraction of the total coverage on the surface, ϕ, is able to migrate some distance to the favourable sites where they nucleate. The Pb atoms scatter in phase with the substrate Ni atoms so that (110) intensity does not follow the parabolic hollow site drop. The nucleation stops when the number of Pb atoms in the region is so large that total energy is minimized when additional atoms adsorb in the hollow sites. We denote this critical coverage for change of adsorption sites by θ^*. For total coverages, $\theta < \theta^*$, the scattering amplitude of the (110) peak from a surface FCC Ni unit cell is given by

$$A = 2\tfrac{1}{2} D_{Ni} f_{Ni} + \phi 2\theta D_{Pb} f_{Pb} - (1 - \phi) 2\theta D_{Pb} f_{Pb}. \tag{8}$$

The first term gives the contribution from the Ni substrate. The second and third terms give the contributions from Pb atoms adsorbing in Ni and hollow sites respectively. The factor of two associated with θ and θ^* comes from the definition that $\theta = 0.5$ for a half monolayer. For $\theta > \theta^*$

$$A = 2\tfrac{1}{2} D_{Ni} f_{Ni} + \phi 2\theta^* D_{Pb} f_{Pb} - (1 - \phi) 2\theta^* D_{Pb} f_{Pb} - 2(\theta - \theta^*) D_{Pb} f_{Pb} \tag{9}$$

where the second and third terms arise from Pb atoms adsorbing in the Ni sites and the hollow sites respectively before θ^* is reached. The fourth term gives the contribution from Pb atoms adsorbing in the hollow sites after θ^* is reached. Normalizing the intensity by the signal of an undosed Ni surface, we obtain

$$I(\theta)/I(0) = (1 + \phi 2\theta (D_{Pb}/D_{Ni}) f_{Pb}/f_{Ni} - (1 - \phi) 2\theta (D_{Pb}/D_{Ni}) f_{Pb}/f_{Ni})^2 \tag{10}$$

for $\theta < \theta^*$ and

$$I(\theta)/I(0) = (1 + \phi 2\theta^* (D_{Pb}/D_{Ni}) f_{Pb}/f_{Ni} - (1 - \phi) 2\theta (D_{Pb}/D_{Ni}) f_{Pb}/f_{Ni}$$
$$- 2(\theta - \theta^*)(D_{Pb}/D_{Ni}) f_{Pb}/f_{Ni})^2 \tag{11}$$

for $\theta > \theta^*$. When the substrate temperature is below 75 °C, both ϕ and θ^* are zero and (10) and (11) and reduce to (4). We take the maximum of the experimental (110) relative intensity to be θ^* and fit the data with ϕ being the only parameter. The fits are shown as lines in figure 5. The model gives an increase of ϕ and θ^* with temperature as expected

and fits the data qualitatively. The failure to give a quantitatively good fit should not be a disappointment due to the crudeness of the model. In particular, the abrupt crossover between (10) and (11) seems unphysical.

Such a model can qualitatively explain a number of observations of the experiment. With increasing temperature, the Pb atoms are more mobile, and a greater fraction of them can move to the Ni sites around the pinning sites. This leads to the observed greater increase in the (110) intensity at higher temperature for low coverages. Near the saturation coverage, the number of pinning sites is small relative to the total number of adsorbed Pb atoms. Thus as temperature is increased to $350\,^\circ$C at $\theta = 0.47$, the (110) intensity increases because some of the Pb atoms at Ni sites can rearrange themselves into hollow sites to reduce strains with neighbouring Pb atoms. They scatter in phase with the majority of the Pb atoms in the monolayer, giving higher (110) intensity.

By only considering the possible models that can account for an initial increase in the (110) intensity, Pb atoms adsorbing equally in domains with only one particular bridge site should also be a candidate. However, the inability of this model to produce a minimum of zero for the (110) intensity rules out its plausibility.

5. Discussion

Besides the determination of adsorption sites, it is interesting to interpret our results for the domain size as a function of coverage. Accordingly, we fit our data for the (100) ordering peak, while the $c(2 \times 2)$ phase is the only structure on the surface, with a $L^{3/2}$ convoluted with the instrumental resolution as lines in figure 3. This lineshape fits the data well for our entire range of peaks with widths in the range 0.012^{-1}–0.08 Å^{-1}, suggesting that a scaling description of the domain growth is appropriate. (Note that any model diffraction lineshape for two-dimensional patches should decay as q^{-3} in the wings of the diffraction peak (Porod's law). $L^{3/2}$ obeys this requirement, but the lineshape used in another domain growth experiment, [2], does not.)

If the average domain size $\bar{r}$, grows as a power law with coverage θ as $\bar{R} \sim \theta^n$, then the growth exponent n can be extracted from a log–log plot of the reciprocal peak width ξ^{-1} against θ. Only our room-temperature results are used, because they provide a sufficient dynamic range for analysis. Figure 6(a) shows a growth exponent n of the order of 2.7. Such a high value for the growth exponent is not predicted by any known models.

One similar study of the scaling of domain size with coverage was performed on Ag on Ge(111) by Zuo and Wendelken [2, 3]. They found growth exponent n in the range of 0.20–0.35 for temperatures of 350–450$\,^\circ$C. Furthermore, in their experiment, the adsorbate ordering peak was observable at much lower coverages. We believe that the reason for the difference between this and the present experiments is in the mobility of the adsorbed atoms. In the present work, the temperature is much lower than the 200$\,^\circ$C at which Pb has a significant mobility on Ni [9]. For Ag on Ge(111), Busch and Henzler [11] have reported significant time dependent annealing of diffraction peaks between 420 and 480 K, at least 150 K below the work of Zuo and Wendelken. It is therefore likely that the size distribution measured by Zuo and Wendelken reflects the equilibrium properties of their system. The thermodynamic state of an adsorbed film of submonolayer coverage, θ, on an infinite surface would be a condensed island, of essentially infinite extent, occupying a fraction $\sim \theta$ of the surface, with a low-density lattice gas occupying the remaining $\sim (1-\theta)$. In such a case, the adsorbate diffraction peak would be resolution limited. Since Zuo and Wendelken observe broader peaks at lower coverage, it is likely that the smaller islands initially grow at favourable sites, arising from substrate heterogeneity.
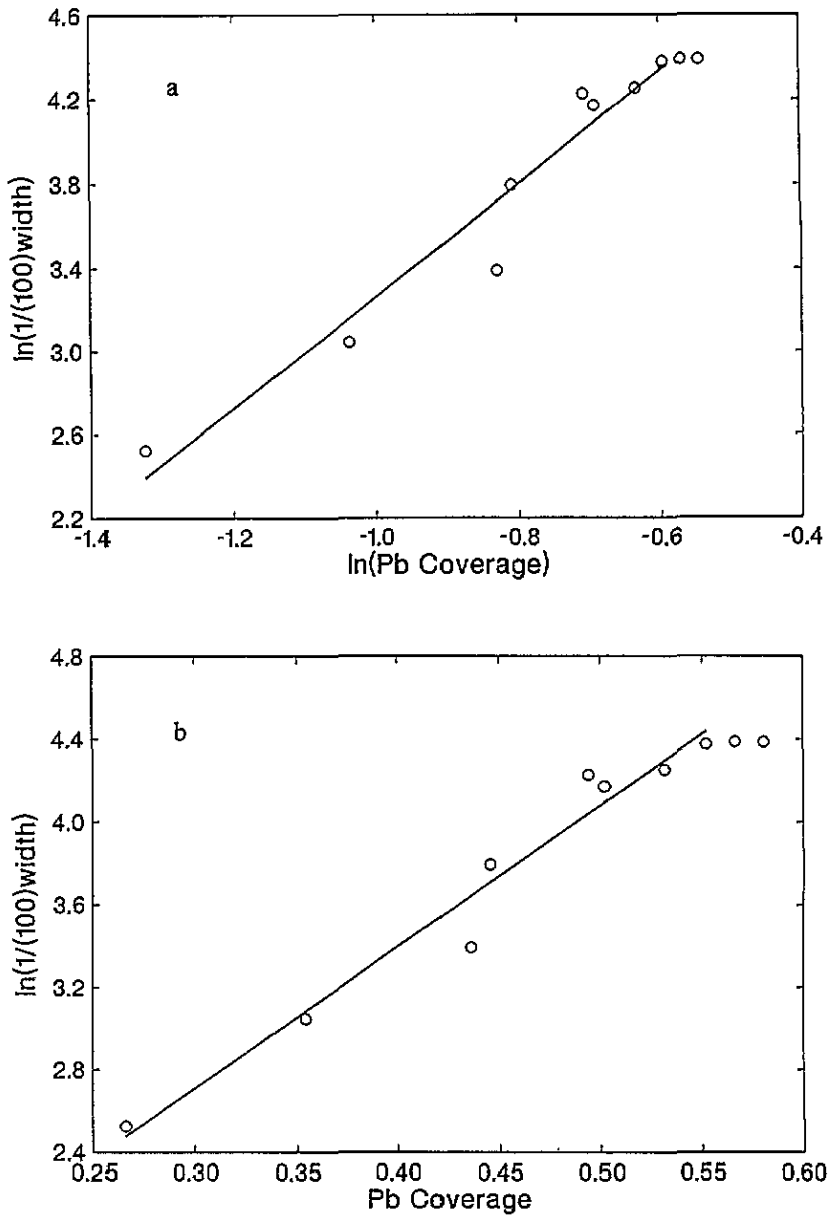
Figure 6. A test of the growth law at room temperature: (*a*) ln(1/(100) width) against ln(Pb coverage) to test power law growth; (*b*) ln(1/(100) width) against Pb coverage to test exponential growth.

An alternative view, with slightly more theoretical foundation, is an extension of Family and Meakin's theory of droplet growth [12]. Our domains on a surface correspond to two-dimensional droplets in a two-dimensional space. The theory is not directly applicable because no degeneracy is considered in the droplet problem. Yet we take its prediction as a crude suggestions to test for other growth laws in our system. According to the theory, the average domain size should grow exponentially with coverage. We plot in figure 6(*b*) the

logarithm of the reciprocal of (100) peak width as a function of coverage using the same set of data as in figure 6(a). The data fit as exponential growth law just as well as a power law. Thus no conclusive verification of the domain growth mode is possible at this stage. Related models have been reviewed by Evans [13].

In conclusion, we have presented a detailed description of the epitaxial growth of the Pb/Ni(001)–c(2 × 2) system with the use of two complementary diffraction peaks, namely, an adsorbate–substrate and an adsorbate–adsorbate interference peak. Pb atoms change from hollow site to non-hollow site growth as coverage increases. Even though part of the growth, particularly the commensurate growth, is somewhat intuitive, it is still important that this is confirmed experimentally in an unambiguous manner by the two-peak analysis. No existing theory can explain the scaling and power law or exponential growth mode, presumably due to the degeneracy of domains. High-temperature deposition exhibits a curious constructive interference between substrate and adsorbates, unexpected from the hollow site growth in the intensity of the non-ordering peak. One possible model that is consistent with all observations is the aggregation of Pb atoms at sites in line with Ni atoms around pinning centres.

References

[1] Zabel H and Robinson I K (ed) 1992 *Surface X-Ray and Neutron Scattering* (Berlin: Springer)
[2] Zue J-K and Wendelken J F 1991 *Phys. Rev. Lett.* **66** 2227
[3] Zue J-K and Wendelken J F 1991 *Appl. Surf. Sci.* **48/49** 366
[4] Stephens P W, End P J and Tse T 1993 *Rev. Sci. Instrum.* **64** 374
[5] Eng P J 1991 *PhD Dissertation* State University of New York at Stony Brook
[6] Blakely J M, Kim J S and Potter H C 1970 *J. Appl. Phys.* **41** 2693
[7] Andrews S R and Cowley R A 1985 *J. Phys. C: Solid State Phys.* **18** 6427
[8] Robinson I K 1986 *Phys. Rev.* B **33** 3830
[9] Eng P J, Stephens P W and Tse T 1992 *Phys. Rev.* B **46** 5024
[10] Tse T and Stephens P W 1993 unpublished
[11] Busch H and Henzler M 1990 *Phys. Rev.* B **41** 4891
[12] Family F and Meakin P 1988 *Phys. Rev. Lett.* **61** 428
[13] Evans J W 1993 *Rev. Mod. Phys.* **65** 1281